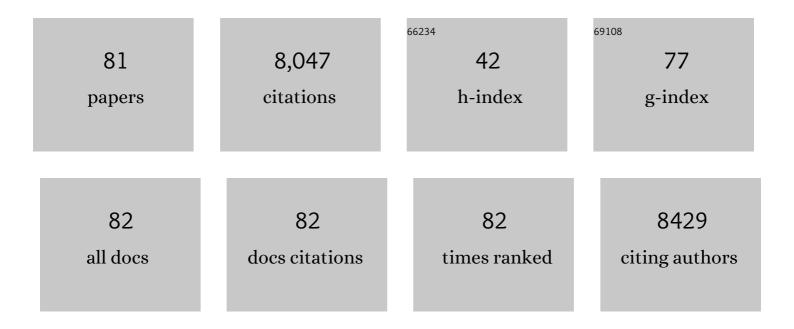
Joseph A Frank

List of Publications by Year in descending order

Source: https://exaly.com/author-pdf/1742543/publications.pdf Version: 2024-02-01



#	Article	IF	CITATIONS
1	Magnetodendrimers allow endosomal magnetic labeling and in vivo tracking of stem cells. Nature Biotechnology, 2001, 19, 1141-1147.	9.4	1,016
2	Encephalitogenic potential of the myelin basic protein peptide (amino acids 83–99) in multiple sclerosis: Results of a phase II clinical trial with an altered peptide ligand. Nature Medicine, 2000, 6, 1167-1175.	15.2	783
3	Clinically Applicable Labeling of Mammalian and Stem Cells by Combining Superparamagnetic Iron Oxides and Transfection Agents. Radiology, 2003, 228, 480-487.	3.6	650
4	Using gadolinium-enhanced magnetic resonance imaging lesions to monitor disease activity in multiple sclerosis. Annals of Neurology, 1992, 32, 758-766.	2.8	351
5	Serial gadolinium-enhanced magnetic resonance imaging scans in patients with early, relapsing-remitting multiple sclerosis: Implications for clinical trials and natural history. Annals of Neurology, 1991, 29, 548-555.	2.8	306
6	Disrupting the blood–brain barrier by focused ultrasound induces sterile inflammation. Proceedings of the United States of America, 2017, 114, E75-E84.	3.3	306
7	H215O PET validation of steady-state arterial spin tagging cerebral blood flow measurements in humans. Magnetic Resonance in Medicine, 2000, 44, 450-456.	1.9	297
8	Functional Magnetic Resonance Imaging Brain Mapping in Psychiatry: Methodological Issues Illustrated in a Study of Working Memory in Schizophrenia. Neuropsychopharmacology, 1998, 18, 186-196.	2.8	293
9	Noise reduction in 3D perfusion imaging by attenuating the static signal in arterial spin tagging (ASSIST). Magnetic Resonance in Medicine, 2000, 44, 92-100.	1.9	293
10	Correction for vascular artifacts in cerebral blood flow values measured by using arterial spin tagging techniques. Magnetic Resonance in Medicine, 1997, 37, 226-235.	1.9	289
11	Synthesis and relaxometry of high-generation (G = 5, 7, 9, and 10) PAMAM dendrimer-DOTA-gadolinium chelates. Journal of Magnetic Resonance Imaging, 1999, 9, 348-352.	1.9	234
12	Clinical imaging in regenerative medicine. Nature Biotechnology, 2014, 32, 804-818.	9.4	207
13	Magnetic Intracellular Labeling of Mammalian Cells by Combining (FDA-Approved) Superparamagnetic Iron Oxide MR Contrast Agents and Commonly Used Transfection Agents. Academic Radiology, 2002, 9, S484-S487.	1.3	200
14	Multislice imaging of quantitative cerebral perfusion with pulsed arterial spin labeling. Magnetic Resonance in Medicine, 1998, 39, 825-832.	1.9	153
15	Perfusion imaging with compensation for asymmetric magnetization transfer effects. Magnetic Resonance in Medicine, 1996, 35, 70-79.	1.9	150
16	Increases in soluble VCAM-1 correlate with a decrease in MRI lesions in multiple sclerosis treated with interferon ?-1b. Annals of Neurology, 1997, 41, 669-674.	2.8	149
17	Frequency dependence of MR relaxation times II. Iron oxides. Journal of Magnetic Resonance Imaging, 1993, 3, 641-648.	1.9	106
18	Hepatic hemosiderosis in non-human primates: Quantification of liver iron using different field strengths. Magnetic Resonance in Medicine, 1997, 37, 530-536.	1.9	89

JOSEPH A FRANK

#	Article	IF	CITATIONS
19	Short- vs. long-circulating magnetoliposomes as bone marrow-seeking MR contrast agents. Journal of Magnetic Resonance Imaging, 1999, 9, 329-335.	1.9	84
20	Serial contrast-enhanced magnetic resonance imaging in patients with early relapsing-remitting multiple sclerosis: Implications for treatment trials. Annals of Neurology, 1994, 36, S86-S90.	2.8	80
21	Radiological–pathological correlation of diffusion tensor and magnetization transfer imaging in a closed head traumatic brain injury model. Annals of Neurology, 2016, 79, 907-920.	2.8	79
22	Study of relapsing remitting experimental allergic encephalomyelitis SJL mouse model using MION-46L enhanced in vivo MRI: Early histopathological correlation. Journal of Neuroscience Research, 1998, 52, 549-558.	1.3	78
23	Leukodystrophy in patients with ovarian dysgenesis. Annals of Neurology, 1997, 41, 654-661.	2.8	73
24	Fast 3D functional magnetic resonance imaging at 1.5 T with spiral acquisition. Magnetic Resonance in Medicine, 1996, 36, 620-626.	1.9	72
25	Reproducibility of Proton Magnetic Resonance Spectroscopic Imaging in Patients with Schizophrenia. Neuropsychopharmacology, 1998, 18, 1-9.	2.8	69
26	Abnormal neurogenesis and cortical growth in congenital heart disease. Science Translational Medicine, 2017, 9, .	5.8	69
27	Superparamagnetic iron oxide nanoparticles for direct labeling of stem cells and <i>in vivo</i> MRI tracking. Contrast Media and Molecular Imaging, 2016, 11, 55-64.	0.4	68
28	3-dimensional functional imaging of human brain using echo-shifted FLASH MRI. Magnetic Resonance in Medicine, 1994, 32, 150-155.	1.9	65
29	Multislice perfusion imaging in human brain using the C-FOCI inversion pulse: Comparison with hyperbolic secant. Magnetic Resonance in Medicine, 1999, 42, 1098-1105.	1.9	64
30	Temporally distinct myeloid cell responses mediate damage and repair after cerebrovascular injury. Nature Neuroscience, 2021, 24, 245-258.	7.1	64
31	A comparison of fast MR scan techniques for cerebral activation studies at 1.5 Tesla. Magnetic Resonance in Medicine, 1998, 39, 61-67.	1.9	63
32	Investigation of Cellular and Molecular Responses to Pulsed Focused Ultrasound in a Mouse Model. PLoS ONE, 2011, 6, e24730.	1.1	60
33	Perfusion imaging of the human brain at 1.5 T using a single-shot EPI spin tagging approach. Magnetic Resonance in Medicine, 1996, 36, 219-224.	1.9	59
34	Effect of magnetization transfer on the measurement of cerebral blood flow using steady-state arterial spin tagging approaches: A theoretical investigation. Magnetic Resonance in Medicine, 1997, 37, 501-510.	1.9	58
35	Correspondence of closest gradient Voxels—A robust registration algorithm. Journal of Magnetic Resonance Imaging, 1997, 7, 410-415.	1.9	55
36	Focused ultrasound with microbubbles induces sterile inflammatory response proportional to the blood brain barrier opening: Attention to experimental conditions. Theranostics, 2018, 8, 2245-2248.	4.6	55

Joseph A Frank

#	Article	IF	CITATIONS
37	Reproducibility of human 3D fMRI brain maps acquired during a motor task. , 1996, 4, 113-121.		54
38	MRI and histological evaluation of pulsed focused ultrasound and microbubbles treatment effects in the brain. Theranostics, 2018, 8, 4837-4855.	4.6	53
39	Functional MR of the kidney. Magnetic Resonance in Medicine, 1991, 22, 319-323.	1.9	49
40	Frequency dependence of MR relaxation times I. Paramagnetic ions. Journal of Magnetic Resonance Imaging, 1993, 3, 637-640.	1.9	45
41	Chlorotoxin—A Multimodal Imaging Platform for Targeting Glioma Tumors. Toxins, 2018, 10, 496.	1.5	45
42	Time series for modelling counts from a relapsing-remitting disease: Application to modelling disease activity in multiple sclerosis. Statistics in Medicine, 1994, 13, 453-466.	0.8	43
43	Diffusion Tensor Imaging Reveals Acute Subcortical Changes after Mild Blast-Induced Traumatic Brain Injury. Scientific Reports, 2014, 4, 4809.	1.6	43
44	Pulsed Focused Ultrasound Pretreatment Improves Mesenchymal Stromal Cell Efficacy in Preventing and Rescuing Established Acute Kidney Injury in Mice. Stem Cells, 2015, 33, 1241-1253.	1.4	42
45	Noninvasive pulsed focused ultrasound allows spatiotemporal control of targeted homing for multiple stem cell types in murine skeletal muscle and the magnitude of cell homing can be increased through repeated applications. Stem Cells, 2013, 31, 2551-2560.	1.4	41
46	In vivo imaging of sterile microglial activation in rat brain after disrupting the blood-brain barrier with pulsed focused ultrasound: [18F]DPA-714 PET study. Journal of Neuroinflammation, 2019, 16, 155.	3.1	40
47	Improving the therapeutic efficacy of mesenchymal stromal cells to restore perfusion in critical limb ischemia through pulsed focused ultrasound. Scientific Reports, 2017, 7, 41550.	1.6	34
48	Blood–brain barrier opening by intracarotid artery hyperosmolar mannitol induces sterile inflammatory and innate immune responses. Proceedings of the National Academy of Sciences of the United States of America, 2021, 118, .	3.3	33
49	Localized echo-volume imaging methods for functional MRI. Journal of Magnetic Resonance Imaging, 1997, 7, 371-375.	1.9	31
50	Incorporation of Lactate Measurement in Multi-Spin-Echo Proton Spectroscopic Imaging. Magnetic Resonance in Medicine, 1995, 33, 101-107.	1.9	30
51	First Noncovalently Bound Calix[4]arene-GdIII-Albumin Complex. Angewandte Chemie - International Edition, 2000, 39, 1641-1643.	7.2	27
52	Quantitation of regional cerebral blood flow increases during motor activation: A multislice, steady-state, arterial spin tagging study. Magnetic Resonance in Medicine, 1999, 42, 404-407.	1.9	26
53	Optimization of fast acquisition methods for whole-brain relative cerebral blood volume (rCBV) mapping with susceptibility contrast agents. Journal of Magnetic Resonance Imaging, 1999, 9, 233-239.	1.9	24
54	Dynamic Enhanced Magnetic Resonance Imaging of Testicular Perfusion in the Rat. Journal of Urology, 1993, 149, 1195-1197.	0.2	23

#	Article	IF	CITATIONS
55	Abnormal Injury Response in Spontaneous Mild Ventriculomegaly Wistar Rat Brains: A Pathological Correlation Study of Diffusion Tensor and Magnetization Transfer Imaging in Mild Traumatic Brain Injury. Journal of Neurotrauma, 2017, 34, 248-256.	1.7	22
56	Mesenchymal stromal cell potency to treat acute kidney injury increased by ultrasoundâ€activated interferonâ€Î³/interleukinâ€10 axis. Journal of Cellular and Molecular Medicine, 2018, 22, 6015-6025.	1.6	22
57	Physicochemical characterization of ferumoxytol, heparin and protamine nanocomplexes for improved magnetic labeling of stem cells. Nanomedicine: Nanotechnology, Biology, and Medicine, 2017, 13, 503-513.	1.7	21
58	Reply to Silburt et al.: Concerning sterile inflammation following focused ultrasound and microbubbles in the brain. Proceedings of the National Academy of Sciences of the United States of America, 2017, 114, E6737-E6738.	3.3	20
59	Neuroinflammation associated with ultrasound-mediated permeabilization of the blood–brain barrier. Trends in Neurosciences, 2022, 45, 459-470.	4.2	19
60	Failure of Intravenous or Intracardiac Delivery of Mesenchymal Stromal Cells to Improve Outcomes after Focal Traumatic Brain Injury in the Female Rat. PLoS ONE, 2015, 10, e0126551.	1.1	15
61	Molecular and histological effects of MR-guided pulsed focused ultrasound to the rat heart. Journal of Translational Medicine, 2017, 15, 252.	1.8	14
62	The Proteomic Effects of Pulsed Focused Ultrasound on Tumor Microenvironments of Murine Melanoma and Breast Cancer Models. Ultrasound in Medicine and Biology, 2019, 45, 3232-3245.	0.7	14
63	On the detection of cerebral metabolic depression in experimental traumatic brain injury using Chemical Exchange Saturation Transfer (CEST)-weighted MRI. Scientific Reports, 2018, 8, 669.	1.6	13
64	Anti-inflammatory drugs suppress ultrasound-mediated mesenchymal stromal cell tropism to kidneys. Scientific Reports, 2017, 7, 8607.	1.6	11
65	Ultrasound-Mediated Microbubble Destruction Suppresses Melanoma Tumor Growth. Ultrasound in Medicine and Biology, 2018, 44, 831-839.	0.7	11
66	The Impact of Focused Ultrasound in Two Tumor Models: Temporal Alterations in the Natural History on Tumor Microenvironment and Immune Cell Response. Cancers, 2020, 12, 350.	1.7	11
67	Effects of large vessels in functional magnetic resonance imaging at 1.5T. International Journal of Imaging Systems and Technology, 1995, 6, 245-252.	2.7	10
68	Controlled Cortical Impact in the Rat. Current Protocols in Neuroscience, 2017, 81, 9.62.1-9.62.12.	2.6	10
69	Cytosolic Ca ²⁺ transients during pulsed focused ultrasound generate reactive oxygen species and cause DNA damage in tumor cells. Theranostics, 2021, 11, 602-613.	4.6	10
70	Application of aziridinium ring opening for preparation of optically active diamine and triamine analogues: highly efficient synthesis and evaluation of DTPA-based MRI contrast enhancement agents. RSC Advances, 2015, 5, 94571-94581.	1.7	9
71	A protocol for assessing subtraction errors of arterial spin-tagging perfusion techniques in human brain. Magnetic Resonance in Medicine, 2000, 43, 896-900.	1.9	8
72	MRâ€guided pulsed focused ultrasound improves mesenchymal stromal cell homing to the myocardium. Journal of Cellular and Molecular Medicine, 2020, 24, 13278-13288.	1.6	7

Joseph A Frank

#	Article	IF	CITATIONS
73	Pulsed-Focused Ultrasound Slows B16 Melanoma and 4T1 Breast Tumor Growth through Differential Tumor Microenvironmental Changes. Cancers, 2021, 13, 1546.	1.7	7
74	Synthesis and characterization of gadolinium—Peptidomimetic complex as an αvβ3 integrin targeted MR contrast agent. Bioorganic and Medicinal Chemistry Letters, 2015, 25, 2056-2059.	1.0	6
75	Pulsed Focal Ultrasound as a Non-Invasive Method to Deliver Exosomes in the Brain/Stroke. Journal of Biomedical Nanotechnology, 2021, 17, 1170-1183.	0.5	6
76	Acoustic Radiation or Cavitation Forces From Therapeutic Ultrasound Generate Prostaglandins and Increase Mesenchymal Stromal Cell Homing to Murine Muscle. Frontiers in Bioengineering and Biotechnology, 2020, 8, 870.	2.0	5
77	Diffusion Tensor Imaging and Chemical Exchange Saturation Transfer MRI Evaluation on the Long-Term Effects of Pulsed Focused Ultrasound and Microbubbles Blood Brain Barrier Opening in the Rat. Frontiers in Neuroscience, 2020, 14, 908.	1.4	3
78	Response to Cardiac regeneration validated. Nature Biotechnology, 2015, 33, 587-587.	9.4	2
79	H215O PET validation of steady-state arterial spin tagging cerebral blood flow measurements in humans. , 2000, 44, 450.		1
80	Cellular Iron Metabolism Studies Demonstate Safety of Magnetic Tracking of Mesenchymal Stem Cells Blood, 2005, 106, 4320-4320.	0.6	0
81	Abstract 19852: Depletion of Neurogenesis within Key Neural Stem/Progenitor Cell Pools Contributes to Brain Immaturity in Congenital Heart Disease. Circulation, 2015, 132, .	1.6	Ο